

CASE FILE  
COPY

RM L55A24

NACA RM L55A24



# RESEARCH MEMORANDUM

FLIGHT AND PREFLIGHT TESTS OF A RAM JET BURNING  
MAGNESIUM SLURRY FUEL AND UTILIZING A SOLID-PROPELLANT  
GAS GENERATOR FOR FUEL EXPULSION

By Walter A. Bartlett, Jr., and William K. Hagginbothom, Jr.

Langley Aeronautical Laboratory  
Langley Field, Va.

NATIONAL ADVISORY COMMITTEE  
FOR AERONAUTICS  
WASHINGTON

April 6, 1955  
Declassified November 8, 1957

## NATIONAL ADVISORY COMMITTEE FOR AERONAUTICS

## RESEARCH MEMORANDUM

FLIGHT AND PREFLIGHT TESTS OF A RAM JET BURNING  
MAGNESIUM SLURRY FUEL AND UTILIZING A SOLID-PROPELLANT  
GAS GENERATOR FOR FUEL EXPULSION

By Walter A. Bartlett, Jr., and William K. Hagginbothom, Jr.

## SUMMARY

A flight investigation was made of a rocket-launched ram-jet engine incorporating a magnesium slurry fuel and a solid-propellant gas generator for fuel expulsion. During the flight, the model accelerated from a Mach number of 1.75 and an altitude of 6,380 feet until burnout at a Mach number of 3.48 and an altitude of 39,200 feet in the time of 15.5 seconds. Maximum values of acceleration (4.6g), air specific impulse (151 seconds), and gross thrust coefficient (0.658) were calculated. Radar contact was lost at an elevation of 84,000 feet, 49 seconds after take-off, with the flight Mach number slightly in excess of 2.

Preflight supersonic free-jet performance tests of the fuel conducted at Mach numbers of 2.03 and 2.26 showed a value of air specific impulse of 156 seconds was obtained at an equivalence ratio of 0.85. The rocket gas generator, developed and used in the fuel-pumping system, was shown to have operated successfully.

## INTRODUCTION

The National Advisory Committee for Aeronautics is conducting a program to develop new high-energy fuels for use in both turbojet and ram-jet applications. One such fuel is a metal slurry fuel, made up of finely divided metal particles suspended in liquid hydrocarbons. The combustion performance of magnesium slurry fuels has been determined in a ram jet mounted in a connected pipe facility at the Lewis High Energy Fuels Laboratory (ref. 1). The results obtained demonstrated that the fuel might be readily and successfully adapted to the type of ram-jet engines used at the Langley Aeronautical Laboratory, of which two designs have

been flight tested using a gaseous hydrocarbon fuel (refs. 2 and 3). Accordingly, a cooperative effort between the Langley and Lewis Laboratories of the NACA was undertaken with the object of successfully flight testing a slurry-fueled ram-jet engine.

The results of the first flight test of a ram jet burning magnesium slurry fuel are presented in this paper. The flight test was made at the Langley Pilotless Aircraft Research Station at Wallops Island, Va. Prior to the flight test, free-jet-performance parameters were obtained in the preflight jet at Wallops Island, Va. Concurrently, a rocket gas generator used to pressurize the fuel-injector system was proven in the preflight tests. These performance parameters are also included in the report.

#### SYMBOLS

$t_f$	time measured from take-off, sec
$p$	static pressure, lb/sq in. abs
$T$	static temperature, $^{\circ}$ R
$A_o$	maximum stream tube area, sq ft
$M$	free-stream Mach number
$S_a$	sonic air specific impulse, $\frac{\text{lb of jet thrust}}{\text{lb of air/sec}}$
$C_T$	thrust coefficient, based on combustion chamber area
$f/a$	fuel-air ratio, weight rate of fuel flow to weight rate of air flow
$\phi$	equivalence ratio, $\frac{\text{Fuel-air ratio}}{\text{Stoichiometric fuel-air ratio}}$
$t_i$	time measured from ignition of gas generator, sec
$\Delta p$	orifice static-pressure drop, lb/sq in. abs
$w_f$	weight rate of fuel flow, lb/sec

$C_D$	external drag coefficient, based on combustion chamber area
$T_s$	stagnation temperature, $^{\circ}$ R
$\phi_M$	ratio of jet impulse at any station to the jet impulse at a sonic station
$p_g$	rocket gas pressure, lb/sq in. gage

#### APPARATUS AND METHODS

##### Flight Model

The model incorporating a Mach number 2.13 design conical shock inlet diffuser is shown as a sketch and a photograph in figures 1(a) and 1(b), respectively. The area ratio of the combined supersonic and subsonic diffuser was 0.461 based on the area at the entrance lip and the combustion-chamber area. The innerbody assembly consisted of the entrance cone, fuel tank, and the burner apparatus. The model was 82.14 inches in length with a  $6\frac{1}{2}$ -inch-diameter combustion chamber, upon which four fins, each with an area of 0.416 square foot, were mounted. An exit nozzle having contraction and expansion area ratios of 0.852 and 0.925 - when referenced to the combustion-chamber area - was attached at the aft end of the combustor.

The combustor was constructed of 3/32 Inconel sheet. The exit nozzle and stabilizing fins were stainless steel. The remainder of the model was constructed of mild steel. The empty model weight was 81.3 pounds.

##### Fuel and Fuel System

The high-energy fuel used in this investigation consisted of magnesium powder suspended in a liquid hydrocarbon. The slurry fuel was developed at the Lewis Flight Propulsion Laboratory, and comprehensive information on its performance as obtained in ground tests is reported in references 1, 4, and 5. The pertinent information on the fuel used in the flight test is as follows:

Specific gravity . . . . .	1.08
Viscosity, centipoises . . . . .	6,800
Particle size (max. diam.), microns . . . . .	1.5

The fuel consisted of 50 percent by weight of each of JP-4 liquid hydrocarbon and magnesium powder. The assay of the magnesium powder was 94 percent pure, with 6 percent magnesium oxide. The weight of fuel carried in the model was 14 pounds.

The use of rocket gas generators in pumping systems has been proposed in references 6 and 7. The method when used in a fuel pumping system was thought to be ideally applicable to this installation because of its small size and weight, and its reliability. The design of the rocket gas generator propellant charge was determined from equations given in references 6 and 7 with certain modifications dictated by experience in propulsion work. These data are presented in the appendix.

The generator (fig. 1(c)), attached to the head cap of the fuel tank, was activated with two 4-delay electric squibs and generated the gases used to expel the fuel from the fuel tank. A British Cordite SU/K propellant grain having a weight of 60 grams with a diameter and length of 1 inch and 3 inches, respectively, was used to generate the gases during the flight test. The generator was made of SAE 4130 steel and had a loaded weight of  $1\frac{1}{4}$  pounds. The rocket gases and fuel were separated by a free-floating piston (fig. 1(d)). A 0.100-inch-diameter flow metering nozzle, located immediately in front of the injector-burner assembly, was used to meter the fuel flow to the engine. A complete description of the injector and flame holder (fig. 1(e)) design is given in reference 1. For the investigation reported herein, however, the length of the burner was cut down from  $7\frac{1}{2}$  inches to 4 inches.

The results of a typical bench test of the gas generator fuel tank assembly are presented in figure 2 as time histories of rocket gas pressure  $p_g$ , static pressure drop  $\Delta p$  across the metering nozzle, and the calculated value of fuel flow rate  $W_f$ . The generator burned for 11.4 seconds producing a maximum value of  $p_g = 710 \text{ lb/sq in. gage}$ . Piston travel, and therefore effective fuel discharge, ended at 13.1 seconds. For this particular test, the propellant grain weighed 78 grams, and had a diameter and length of  $1\frac{1}{16}$  inches and  $3\frac{1}{4}$  inches, respectively.

A magnesium flare was cemented into the flame holder and fired at take-off to serve as an ignitor for the fuel. An aluminum annular ring starting disc, blocking 47 percent of the combustor area was inserted immediately in front of the exit nozzle. The starting disc technique is described in reference 8.

In order to check the performance of the fuel, burner, and starting technique prior to the flight test, preflight tests were conducted with an engine having an inlet similar to the flight test engine in the pre-flight jet of the Langley Pilotless Aircraft Research Station at Wallops Island, Va.

#### Booster Rocket and Adapter

A JATO 3.5-DS-5700 rocket motor was used to accelerate the ram jet to supersonic speed. A cast magnesium alloy coupling fastened to the rocket motor and fitted internally in the ram-jet exit nozzle attached the ram jet to the booster. This coupling was designed to block only 10 percent of the nozzle exit area during the boost period. Four fins, each with an area of  $1\frac{1}{4}$  square feet, were mounted at the rear end of the rocket motor and provided stability of the combination during the boost period. A photograph of the ram jet and coupled booster in place on the launcher prior to firing is shown as figure 3.

#### Measurements

The velocity of the model in flight was measured with a CW Doppler radar. The position of the model in space was determined with NACA modified SCR 584 tracking radar. High-speed manually operated tracking cameras provided information on the behavior of the model during the initial portion of the flight.

Upon completion of the flight test, a radiosonde balloon was released to obtain the pressure and temperature of the atmosphere as a function of altitude. The radiosonde balloon was tracked with NACA modified SCR 584 radar in order to obtain wind velocity at altitude. Values of static pressure  $p$  and static temperature  $T$  obtained from radiosonde data are presented in figure 4 as functions of altitude.

### RESULTS AND DISCUSSION

#### Free Jet Tests

Prior to the flight test, the performance of the fuel, burner, and the starting technique was checked in a free jet in an engine having an inlet similar to the flight engine. Comprehensive data on these subjects, obtained in a connected pipe facility with the same engine, were reported in reference 1. A photograph of the preflight engine mounted in the  $M = 2.03$  free jet, and a sketch showing the configuration tested together

with principal areas are given in figures 5(a) and 5(b), respectively. In this series of tests, helium was used to pressurize the fuel system, thereby forcing the fuel into the combustor.

The results of the preflight performance tests conducted at  $M = 2.03$  and  $2.26$  are presented in figure 6 with air specific impulse  $S_a$  (obtained by the method of ref. 8) against equivalence ratio  $\phi$  for the range of stagnation temperatures  $T_s$  and free-stream static pressures  $p$  indicated. Included in the figure is the theoretical curve for  $S_a$  at  $T_s = 810^\circ R$  obtained from reference 1. Linear increases in  $S_a$  were realized with increasing fuel rate up to a value of  $\phi = 0.815$  with  $S_a = 154$  seconds. Diffuser instability or "buzz" occurred above this value and large increases in fuel rate produced disproportionately small increases in thrust impulse. These tests show that for this configuration a value of  $\phi = 0.815$  should not be exceeded, for satisfactory utilization of the magnesium slurry fuel at these Mach numbers. The weight flow of air was determined for these tests by using the relationship of maximum stream tube area to Mach number given in figure 7. These data were obtained by the experimental method and the one-dimensional-flow analysis that are described in reference 8.

Thrust coefficients  $C_T$  as a function of fuel-air ratio  $f/a$  are presented in figure 8 for  $M = 2.03$  for the indicated values of  $T_s$  and  $p$ . Increases in  $f/a$  gave attendant increases in  $C_T$  up to the point that engine buzz was experienced. At  $M = 2.03$ , a value of  $C_{T_{max}} = 0.86$  was obtained with  $f/a = 0.092$ .

A preflight jet test was then conducted to check the complete fuel system under simulated flight conditions. The test was conducted at  $M = 2.03$  with  $T_s = 800^\circ \pm 10^\circ R$  and  $p = 12.5 \pm 0.2 \text{ lb sq in. abs}$ . The flight fuel tank was connected to the ground test engine (fig. 5(b)) for this test. The results of this test are presented as a time history of  $S_a$  and  $p_g$  in figure 9. Zero time is defined as generator ignition time. A lag of 2.8 seconds occurred before the ram jet ignited while the fuel lines filled with fuel. The engine then "buzzed" for approximately 1.2 seconds while the starting disc burned out before the value of  $S_a$  markedly increased. Maximum values of  $S_a = 129$  seconds were computed with the gas generator pressure =  $1260 \text{ lb/sq in. gage}$ . The gas generator grain burned out at 13 seconds with resultant rapid decay in  $p_g$  and  $S_a$ . The fuel was completely expelled from the tank at the time of 20.7 seconds when combustion ceased.

### Flight Test

The altitude and horizontal range coordinates, as obtained from SCR 584 data, are presented in figure 10 up to the point where radar contact was lost. The altitude-time data are also presented for the powered portion of the flight. The pertinent events and the times at which they occurred in flight are noted on the figure.

The flight Mach number  $M$  of the ram jet is presented in figure 11 as a function of flight time. Doppler velocity data were used in these calculations after appropriate corrections for wind speeds at the various altitudes. The model decelerated from  $M = 1.95$  to  $M = 1.75$  during the ignition phase of the flight. A peak Mach number of 3.48 was reached 21 seconds after take-off. Reduction of the data demonstrated that during this period, the model experienced maximum longitudinal accelerations of  $4.6g$ . The Reynolds number, based on body length, varied between  $72 \times 10^6$  and  $45 \times 10^6$  during the powered portion of the flight. The model then decelerated to  $M = 2.78$  at which time Doppler radar contact was lost. It is interesting to note that when SCR 584 contact was lost at 84,000 feet altitude (see fig. 10), a Mach number slightly in excess of 2 was computed from the data.

The gross thrust coefficient  $C_T$  of the ram-jet engine is presented in figure 12 as a function of Mach number. The net thrust available was obtained from the longitudinal acceleration data, (obtained from Doppler radar) and the mass of the ram jet (with appropriate corrections for changing mass with fuel consumption). The gross thrust coefficient was obtained from the net thrust coefficient and the computed external drag coefficient  $C_D$  also presented in figure 12. The fuel expenditure was determined by assuming a constant fuel rate from generator firing to burnout for an elapsed time of 17.4 seconds. The external drag coefficient  $C_D$  was estimated from theoretical friction and pressure drag on the engine and fins, with experimental values of additive drag of the inlet below design Mach number as obtained from the data of reference 9. A maximum value of  $C_T = 0.65$  was calculated at  $M = 1.8$  for these data.

A time history of  $S_a$  delivered by the ram jet is presented in figure 13. The values of  $S_a$ , at the sonic section of the exit nozzle, were obtained by adding the momentum of the air entering the ram jet to the gross thrust and dividing this quantity by the weight flow of air and the thrust function  $\phi M$  (ref. 10). A maximum value of  $S_a = 151$  seconds was calculated from the data at the time of 16 seconds at  $M = 3.05$ . The calculated values of free-stream stagnation temperature  $T_s$  also presented in figure 13 indicate a maximum value of  $T_s = 1340^\circ R$  was reached at the peak value of  $M$ .

The total fuel load of 14 pounds was considered to have been expended between the times of 3.6 and 21 seconds to produce a gross impulse of 7690 pound-seconds. The ratio of these values demonstrates that an overall value of fuel specific impulse of 549 seconds was obtained and may be compared to that of 200 seconds for solid-propellant rocket fuels, 412 seconds for solid fuel ram jets (ref. 11), and 1050 and 956 seconds for the gaseous hydrocarbon fuel ram jets reported in references 2 and 12. The product of the value of fuel specific impulse and the corresponding fuel specific gravity can be defined as the fuel volume specific impulse. The fuel volume specific impulses thus obtained are 593 seconds for the slurry fuel, 320 seconds for the solid rocket, 530 seconds for solid fuel ram jets, and 307 and 280 seconds for the gaseous hydrocarbon fuels.

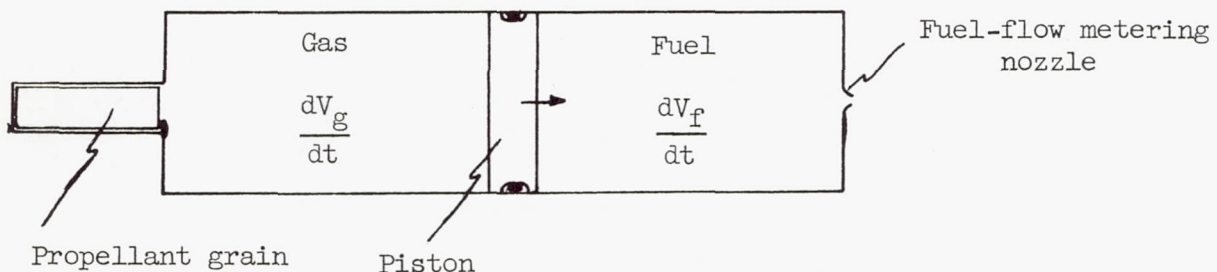
Langley Aeronautical Laboratory,  
National Advisory Committee for Aeronautics,  
Langley Field, Va., January 12, 1955.

## APPENDIX

## DESIGN OF SOLID-PROPELLANT GAS GENERATOR FOR FUEL EXPULSION

## Analysis

In order to utilize a solid-propellant gas generator for fuel expulsion, it is necessary to establish an equilibrium between the rate at which gas is generated by the burning propellant and the rate at which fuel is discharged through a flow metering nozzle. For the case herein reported where a piston serves to transfer energy from the gas to the fuel, as shown diagrammatically in the accompanying illustration, the required equilibrium consists of equating the change in volume of gas to the change in volume of fuel as the piston travels down the cylinder, that is,



$$\frac{dV_g}{dt} = \frac{dV_f}{dt}$$

or

$$Q_g = Q_f \quad (1)$$

where

$Q_g$       volume rate of propellant gas generated, cu in./sec

$Q_f$       volume rate of fuel discharged, cu in./sec

The rate at which gases are generated by combustion of a solid propellant is a function of the amount of propellant grain surface area exposed to

burning and the variation of linear burning rate of the propellant with combustion pressure, and may be expressed as:

$$W_g = \rho_G S r = \rho_G S c p_g^n \quad (2)$$

where

$W_g$  weight rate of propellant gas generation, lb/sec

$\rho_G$  propellant grain density, lb/cu in.

$S$  propellant grain surface area, sq in.

$r$  linear propellant burning rate, in./sec

$p_g$  propellant gas pressure, lb/sq in. abs.

$c$  propellant burning rate coefficient  
 $n$  propellant burning rate exponent

Note: In rocket internal ballistics,  $c$  and  $n$  are factors which satisfy the empirical relation between propellant combustion pressure and burning rate,  $r = cp^n$

On a volumetric basis equation (2) becomes

$$Q_g = \frac{\rho_G S r}{\rho_g'} = \frac{\rho_G S c p_g^n}{\rho_g'} \quad (3)$$

where  $\rho_g'$  is the effective propellant gas density, lb/cu in.

The rate at which fuel is discharged through the metering nozzle primarily depends upon the pressure drop across the nozzle, the nozzle discharge area, and the discharge characteristics of the nozzle, as indicated by

$$Q_f = 144 C A_N \sqrt{\frac{2g}{\rho_f} (p_f - p_b)} \quad (4)$$

where

$C$  nozzle discharge coefficient

$A_N$  nozzle discharge area, sq in.

$\rho_f$  fuel density, lb/cu ft

$p_f$  fuel pressure upstream of metering nozzle, lb/sq in. abs

$p_b$  fuel back pressure downstream of metering nozzle, lb/sq in. abs

$g$  gravitational constant, ft/sec<sup>2</sup>

Since in this analysis a given volume of fuel is displaced by the same volume of gases at a given rate, the duration of fuel discharge must be equal to the duration of gas generation, that is, duration of propellant burning. Thus,

$$t = \frac{l_G}{r} = \frac{V_f}{Q_f} \quad (5)$$

where

$t$  duration, sec

$l_G$  propellant grain burning distance, in.

$V_f$  volume of fuel tank, cu in.

Close inspection of the gas generation equation (3) and fuel discharge equation (4) reveals that, once a particular fuel and propellant are selected, many of the variables in the equations become fixed. For a solid propellant operating at a given pressure,  $\rho_g$ ,  $\rho_g'$ ,  $c$ , and  $n$  are known and constant. In like manner,  $\rho_f$  becomes fixed for a given fuel. This leaves the propellant grain surface area  $S$  and the nozzle discharge area  $A_N$  as the two main design variables which can be adjusted to provide the fuel pressure  $p_f$  necessary to obtain the required fuel flow rate. This relationship between  $S$ ,  $A_N$ , and  $p_f$  may be more clearly demonstrated by further development of equilibrium equation (1)  $Q_g = Q_f$

Substituting equations (3) and (4) into equation (1) yields

$$\frac{\rho_g S c p_g^n}{\rho_g'} = 144 C A_N \sqrt{\frac{2g}{\rho_f} (p_f - p_b)} \quad (6)$$

Once the fuel to be expelled and the propellant to expel it are chosen,  $\rho_G$ ,  $c$ , and  $p_f$  are known and constant, and  $\rho_g'$  is a function of  $p_g$ , that is,  $\rho_g' = k_1 p_g$ . Then, rearranging, equation (6) becomes

$$\frac{S}{A_N} = \frac{144Ck_1}{\rho_G^c p_g} n^{-1} \sqrt{\frac{2g}{\rho_f}} \sqrt{p_f \left(1 - \frac{p_b}{p_f}\right)} \quad (7)$$

Now, in practice,  $p_f$  is equal to  $p_g$  except for a very small frictional loss across the piston. So, letting  $p_f = k_2 p_g$  and

$$K = \frac{144Ck_1 k_2}{\rho_G^c} n^{-1} \sqrt{\frac{2g}{\rho_f}} \quad \text{equation (7) becomes}$$

$$\frac{S}{A_N} = K p_f^{\frac{3}{2} - n} \sqrt{1 - \frac{p_b}{p_f}} \quad (8)$$

#### Design Procedure

The designer of a fuel expulsion system for a free-flight aerodynamic research model is usually confronted with certain space and size limitations which have to be taken into account along with the performance requirements. Practical considerations dictate the size of fuel tank permissible as well as the size of the gas generator unit.

The usual design procedure may be outlined as follows: For the required fuel flow rate and a given tank size, the duration is evident from equation (5). Selection of a propellant and assumption of a suitable operating pressure permits the determination of the propellant burning surface and consequently the grain length and diameter from equations (2) and (5). Once the fuel to be used is selected, knowing the back pressure into which the fuel is to be discharged and assuming a representative value of discharge coefficient, the nozzle discharge area may be determined from equation (4).

Should any of the values of the parameters thus found be unacceptable, adjustment can be made by changing the propellant grain burning surface or the nozzle discharge area or both. Through static testing of the system designed, the value of discharge coefficient for the configuration can be determined experimentally and any discrepancy from the value assumed can be corrected, if necessary.

To illustrate the design procedure, consider the design of a ram-jet fuel expulsion system to meet the following average requirements:

- (1) Fuel tank size: 4.5-inch inside diameter  $\times$  21-inch length  
(333 cu in. free volume)
- (2) Fuel weight flow rate: 1 lb/sec average

Further let magnesium slurry, having a density of 67.8 lb/cu ft, be selected as fuel to be used and Cordite SU/K as the propellant. Pertinent properties of Cordite SU/K propellant are given in the following table:

Grain density, $\rho_G$ , lb/cu in.	0.057
Gas constant, $R$ , $\frac{\text{ft-lb}}{\text{lb-}^{\circ}\text{R}}$	65.9
Adiabatic flame temperature, $T_g$ , $^{\circ}\text{R}$	4493
Burning rate coefficient, $c$	0.00844
Burning rate exponent, $n$	0.54

The average volumetric rate of gas generation and fuel discharge required is  $Q_g = Q_f = \frac{1 \times 1728}{67.8} = 25.5$  cu in./sec. For the given fuel tank size, the duration of fuel discharge is evident from equation (5),

$$t = \frac{V_f}{Q_f} = \frac{333}{25.5} = 13.1 \text{ sec}$$

In order to keep the propellant design within practicable limits, the designer generally selects a reasonable value for combustion gas pressure, high enough to insure steady burning but not so high as to introduce structural problems. For the design under consideration, let  $p_g = 600$  lb/sq in. abs, which, from perfect gas relations, would indicate an ideal gas density as follows:

$$\rho_g = \frac{p_g \times 144}{RT_g \times 1728} = \frac{600 \times 144}{65.9 \times 4493 \times 1728} = 0.000169 \text{ lb/cu in.}$$

In the practical case, heat transfer from the gas being generated to the surrounding metal parts, such as the propellant case, piston assembly, and fuel tank walls, results in considerable loss in gas temperature.

The amount of heat transfer depends upon the system configuration and the burning characteristics of the propellant and, therefore, can vary considerably for different fluid expulsion systems, as indicated in reference 6. Experience has shown that this effect can be accounted for by using an "effective" gas density  $\rho_g'$  in place of the ideal density calculated from the perfect gas relationship. Experimental results of the present investigation indicate that the ratio of effective gas density to the ideal gas density is approximately 3 for the configuration under con-

sideration. Accordingly, assuming  $\frac{\rho_g'}{\rho_g} = 3$ , the effective gas density

would be

$$\rho_g' = 3 \times 0.000169 = 0.000507 \text{ lb/cu in.}$$

Then, solving equation (3) for the value of propellant burning surface required yields

$$S = \frac{Q_g \rho_g'}{\rho_G c p_g n} = \frac{25.5 \times 0.000507}{0.057 \times 0.00844 \times 600^{.54}} = 0.848 \text{ sq in.}$$

In order to obtain as long a burning time as is required, an end-burning propellant configuration will be utilized. To achieve end burning, the entire propellant surface is inhibited except for one end, so that burning of that end surface proceeds linearly down the length of the propellant grain. From the burning surface just determined and the linear burning rate of the propellant, a tentative size and shape of propellant grain may be determined. Thus, the grain diameter  $d_G = \sqrt{\frac{0.848}{0.785}} = 1.04 \text{ inches}$  and grain length  $l_G = tr = 13.1 \times 0.00844 \times 600^{.54} = 3.5 \text{ inches.}$

Having established the gas generation characteristics of the system, the fuel discharge characteristics can be determined easily from equation (4). For the ram-jet application under consideration, the back pressure in the injector assembly against which the fuel is to be expelled from the tank will be approximately 55 lb/sq in. abs. For the piston and guide assembly of the type reported herein, experience has shown the fuel pressure to be approximately 97.5 percent of the gas pressure or, in this case, 585 lb/sq in. abs. Assuming a discharge coefficient of 0.85, the nozzle discharge area can be determined from equation (4),

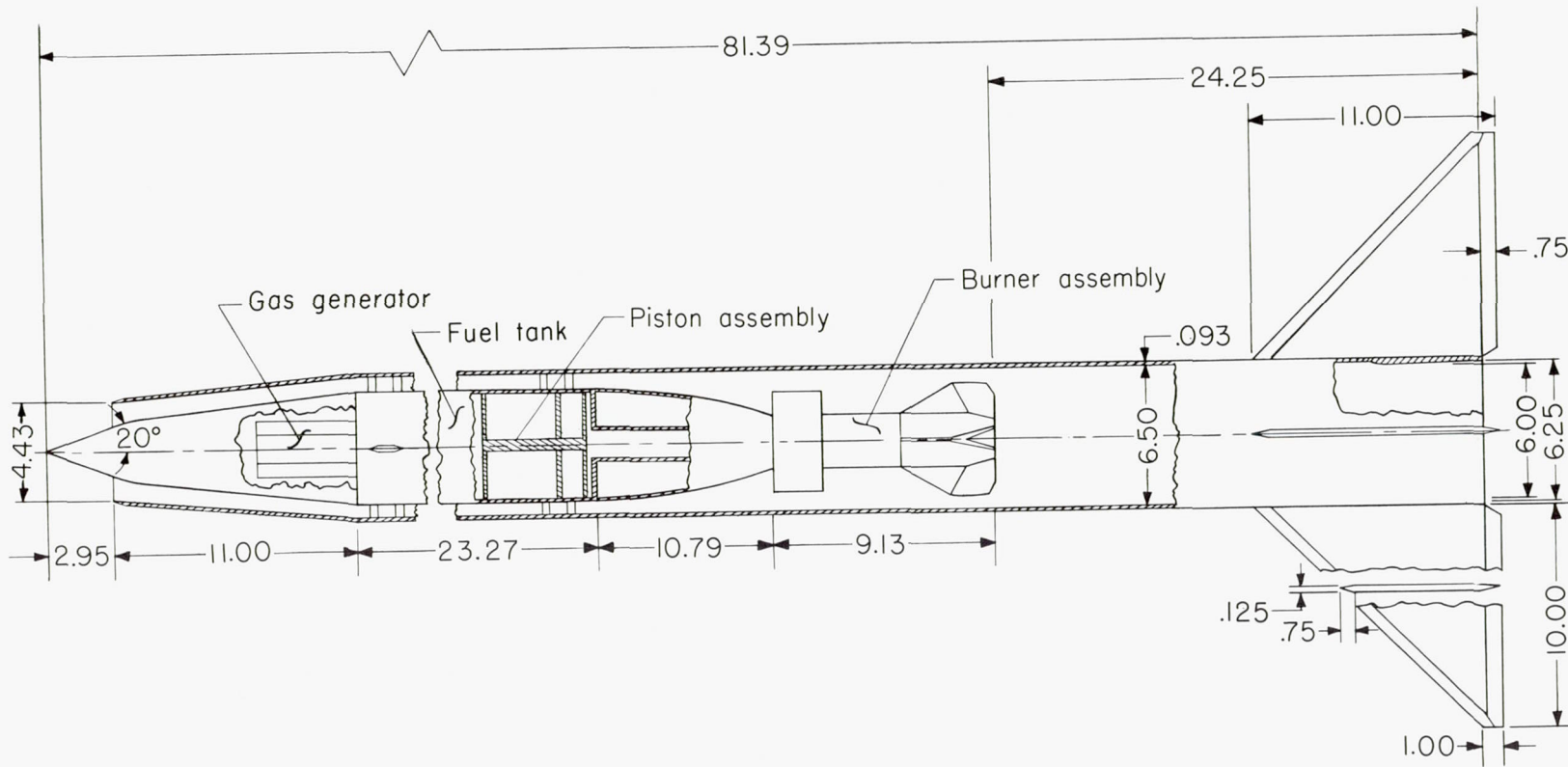
$$A_N = \frac{Q_f}{144C \frac{2g}{\rho_f} (p_f - p_b)} = \frac{25.5}{144 \times 0.85 \frac{64.4}{67.8} (585 - 55)} = 0.00927 \text{ sq in.}$$

Hence, the nozzle discharge diameter required is 0.109 inch.

## REFERENCES

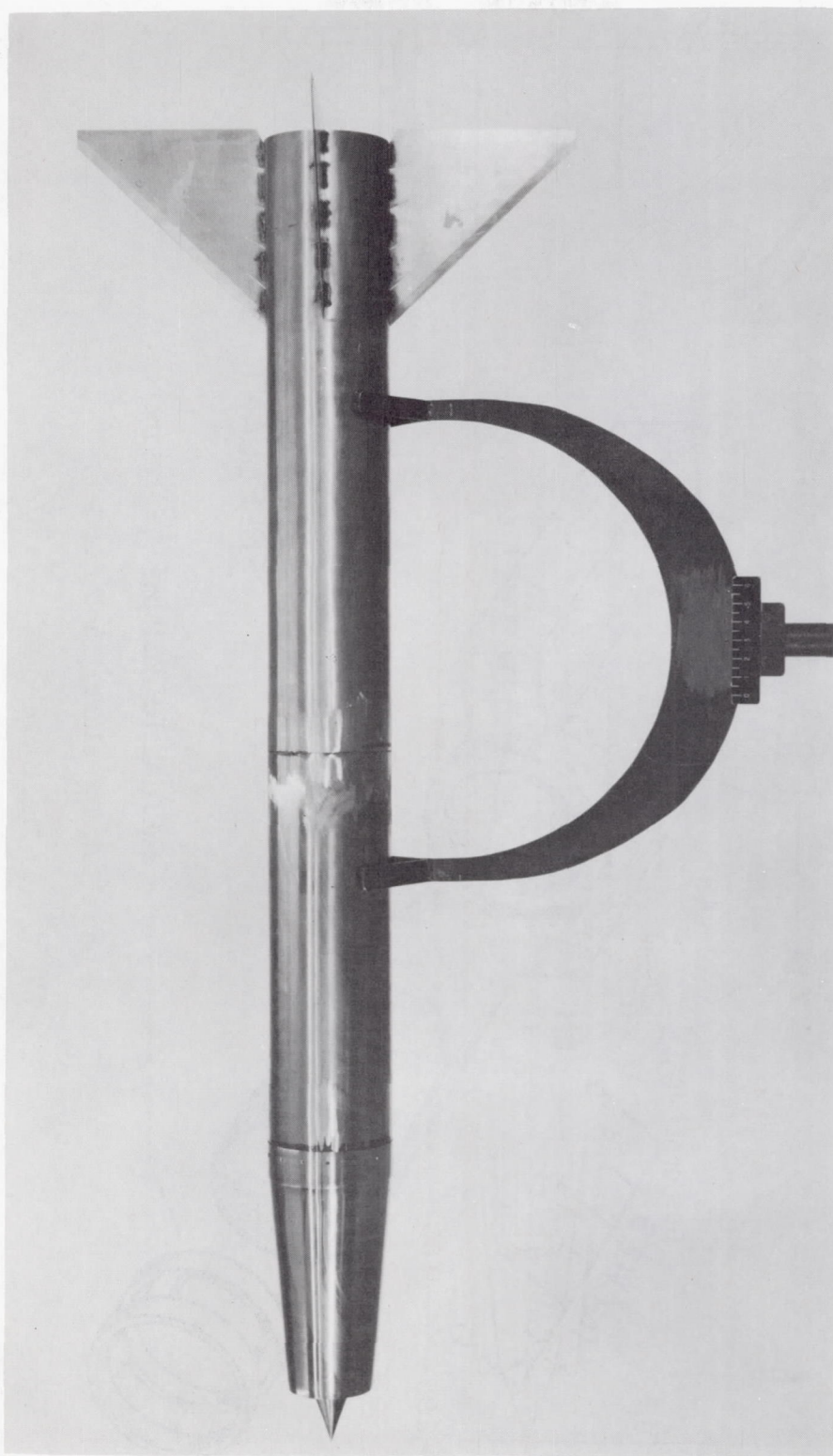
1. Branstetter, J. Robert, Gibbs, James B., and Kaufman, Warner B.: Magnesium-Slurry Combustion Performance in 6.5-Inch-Diameter Ram-Jet Engine Mounted in Connected-Pipe Facility. NACA RM E53E27, 1953.
2. Faget, Maxime A., and Dettwyler, H. Rudolph: Initial Flight Investigation of a Twin-Engine Supersonic Ram Jet. NACA RM L50H10, 1950.
3. Hinners, Arthur H., Jr., and Foland, Douglas H.: Preflight Tests and Flight Performance of a 6.5-Inch-Diameter Ram-Jet Engine. NACA RM L53H28, 1953.
4. Tower, Leonard K., and Branstetter, J. Robert: Combustion Performance Evaluation of Magnesium-Hydrocarbon Slurry Blends in a Simulated Tail-Pipe Burner. NACA RM E51C26, 1951.
5. Lord, Albert M.: An Experimental Investigation of the Combustion Properties of a Hydrocarbon Fuel and Several Magnesium and Boron Slurries. NACA RM E52B01, 1952.
6. Orton, J. W.: Development of a Cordite-Operated Fuel Expulsion System For 7.2-in. Ramjet. Tech. Note No. R.P.D.9, British R.A.E., Dec. 1948.
7. Miller, Eugene, and Olicker, S. D.: Development of 15,000-lb and 90,000-lb Thrust Liquid Propellant Booster Rockets. Res. and Dev. Rep. SPD 270 (Bur. Aero. Contract NOa(s) 9498), the M. W. Kellogg Co., Special Projects Dept. (Jersey City), Mar. 31, 1950.
8. Faget, Maxime A., Watson, Raymond S., and Bartlett, Walter A., Jr.: Free-Jet Tests of a 6.5-Inch-Diameter Ram-Jet Engine at Mach Numbers of 1.81 and 2.00. NACA RM L50L06, 1951.
9. Merlet, Charles F., and Putland, Leonard W.: Flight Determination of the Drag of Conical-Shock Nose Inlets With Various Cowling Shapes and Axial Positions of the Center Body at Mach Numbers From 0.8 to 2.0. NACA RM L54G21a, 1954.
10. Beer, A. C.: An Analytical Approach to Ramjet Design Optimization. Bumblebee Rep. No. 108, The Johns Hopkins Univ., Appl. Phys. Lab., Dec. 1949.
11. Bartlett, Walter A., Jr., and Dettwyler, H. Rudolph: Flight Test of a Radial-Burning Solid-Fuel Ram Jet. NACA RM L52K03, 1952.

12. Dettwyler, H. Rudolph, and Bond, Aleck C.: Flight Performance of a Twin-Engine Supersonic Ram Jet From 2,300 to 67,200 Feet Altitude.  
NACA RM L50L27, 1951.



(a) Sketch of model. All dimensions are in inches.

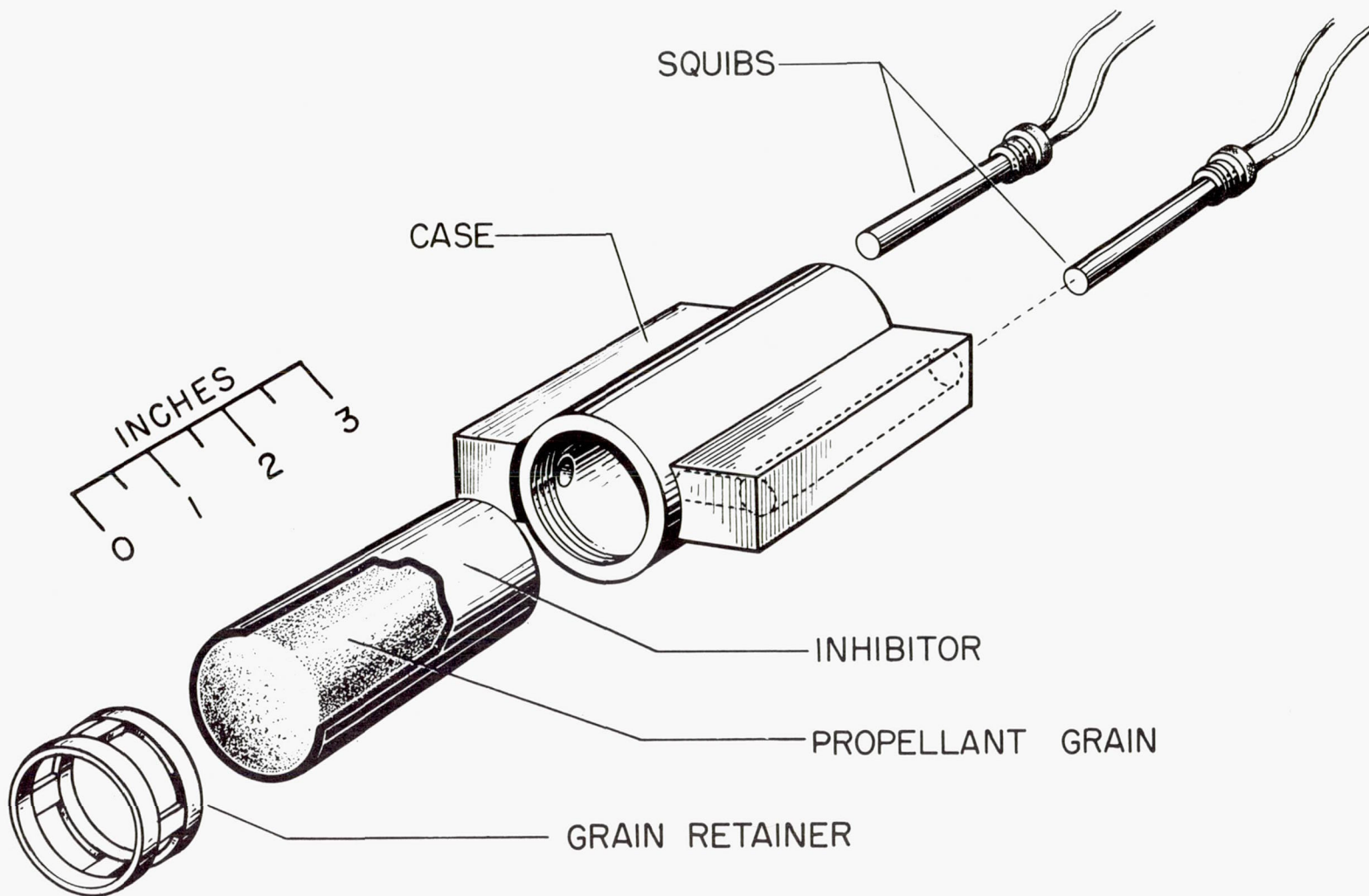
Figure 1.- The slurry fuel ram jet.



L-83601.1

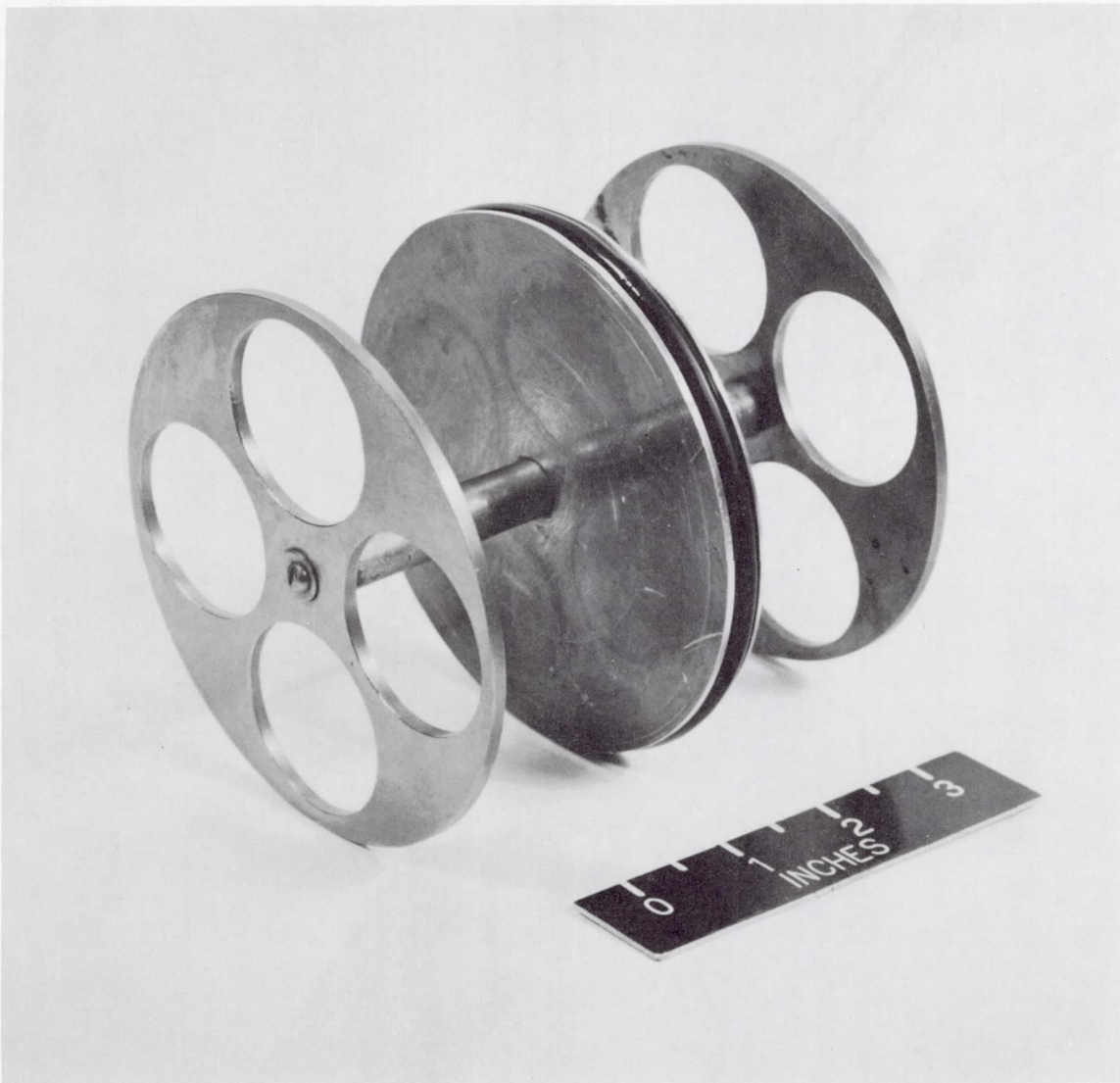
(b) Photograph of model.

Figure 1.- Continued.



(c) The rocket gas generator.

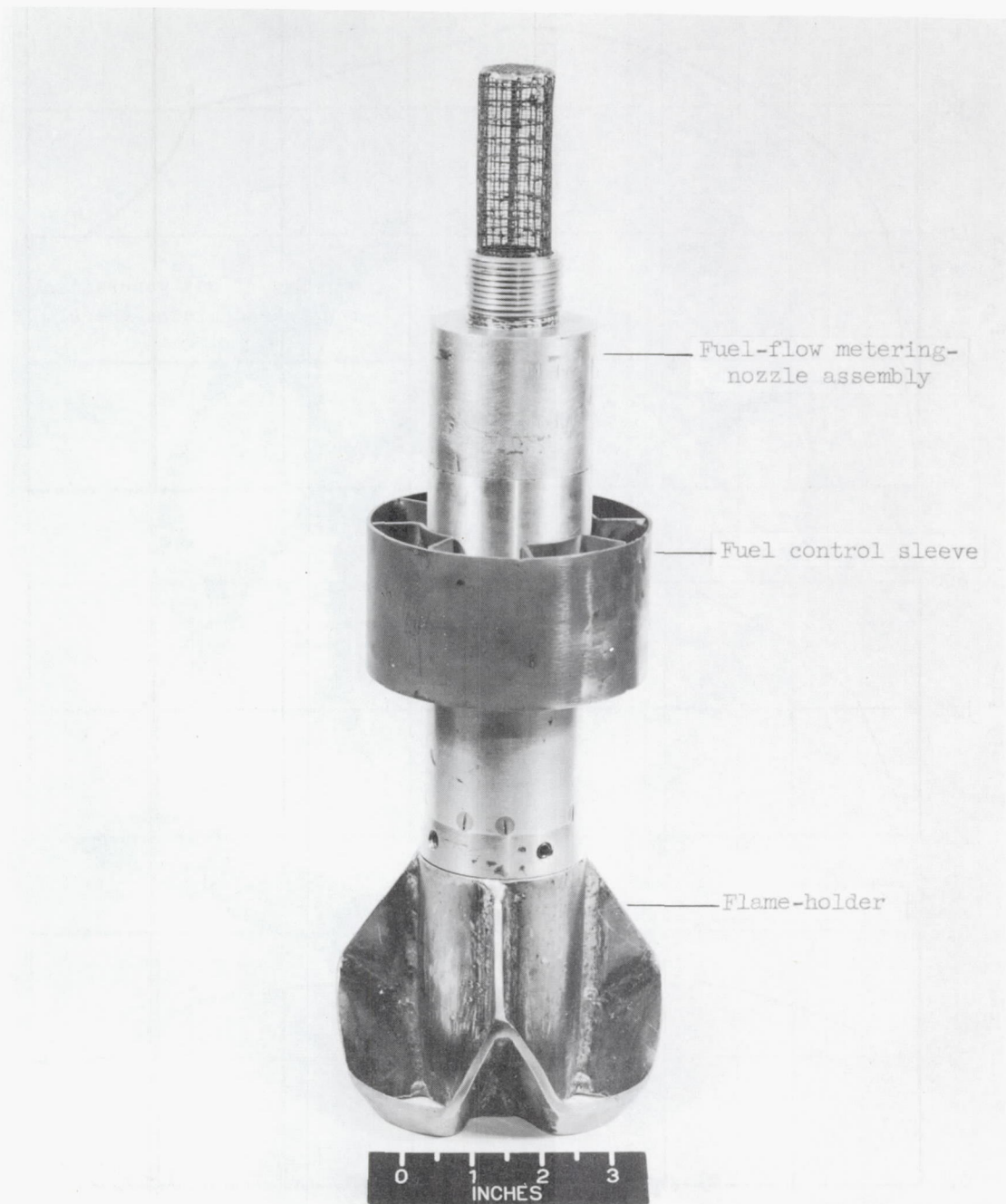
Figure 1.- Continued.



(d) Photograph of piston.

L-83856

Figure 1.- Continued.



(e) The fuel ejector and flame-holder assembly. L-83857-1

Figure 1.- Concluded.

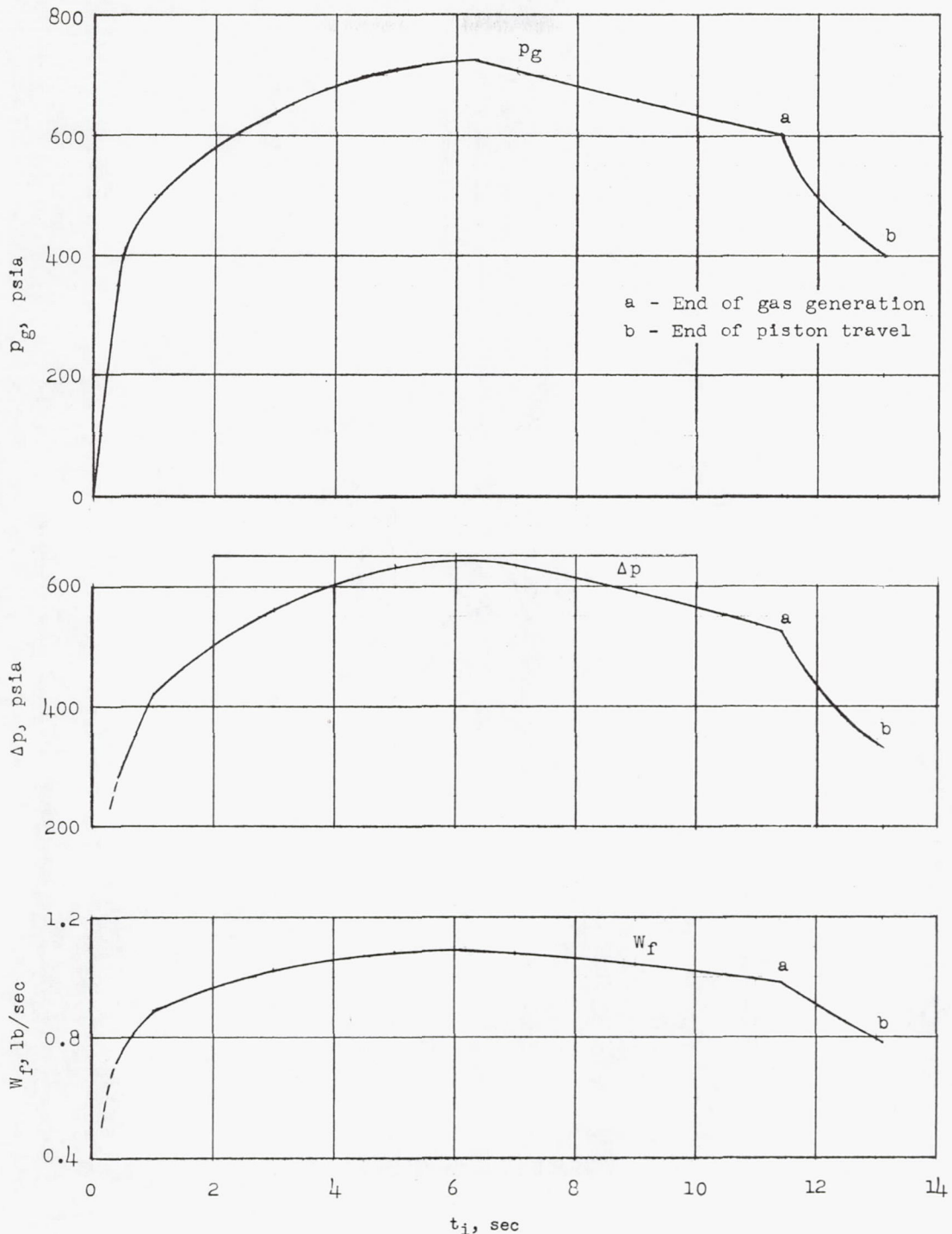
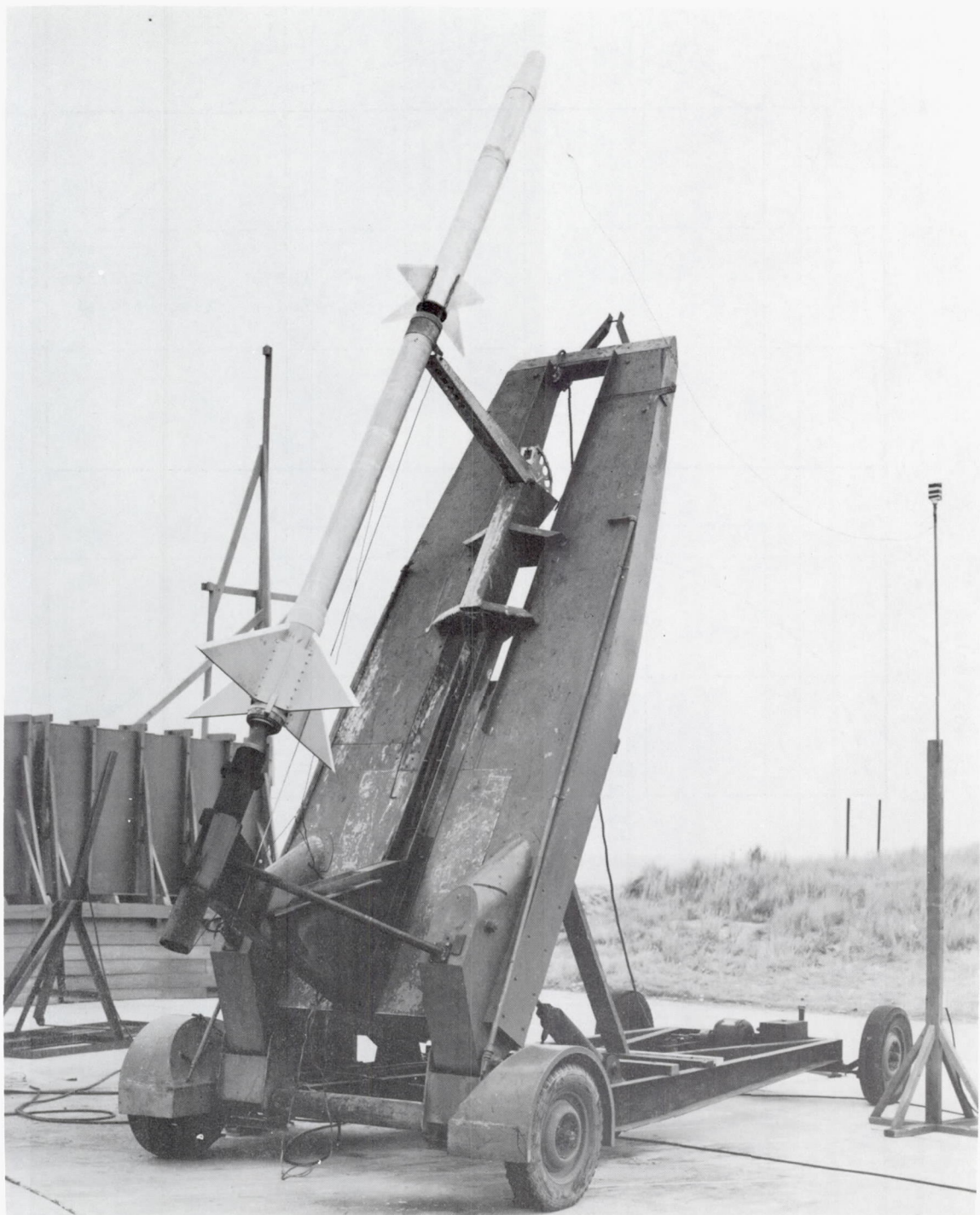


Figure 2.- Time history of propellant gas pressure, metered fuel pressure drop and fuel weight flow for bench test of fuel expulsion system.

Cordite SU/K propellant,  $1\frac{1}{16}$ -inch diameter by  $3\frac{1}{4}$ -inch long.



L-83858.1

Figure 3.- The test model and booster in the launching attitude.

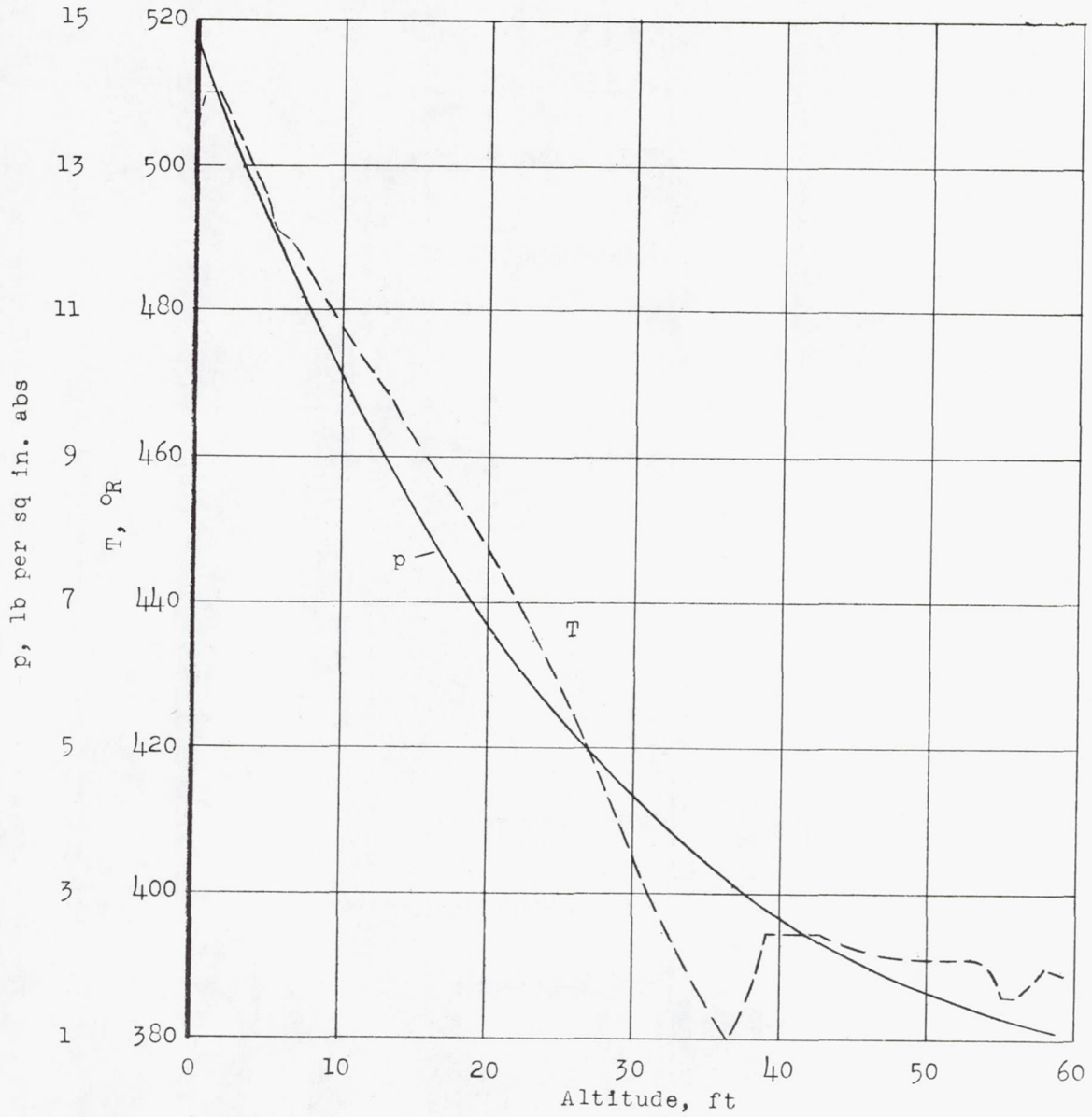
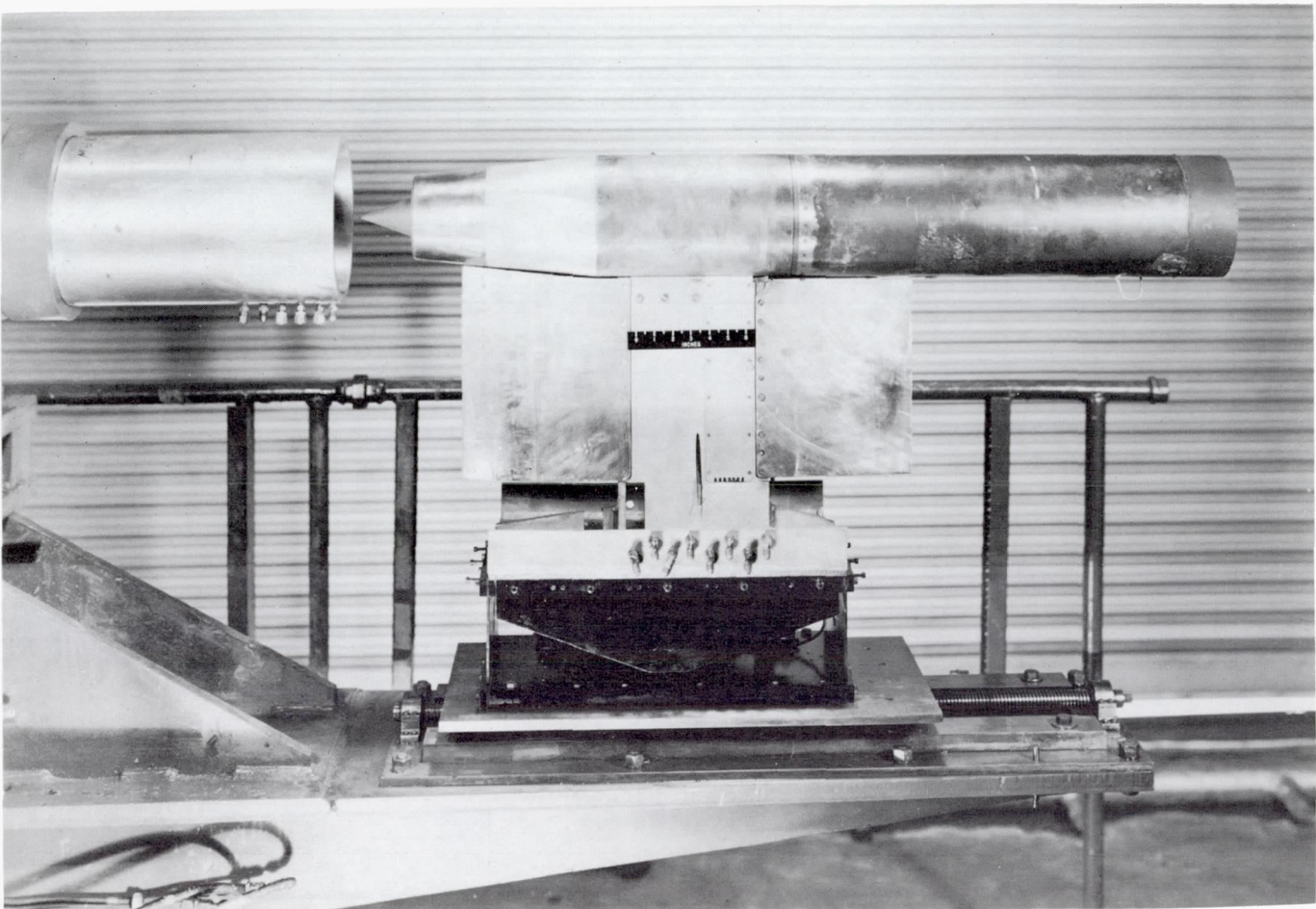


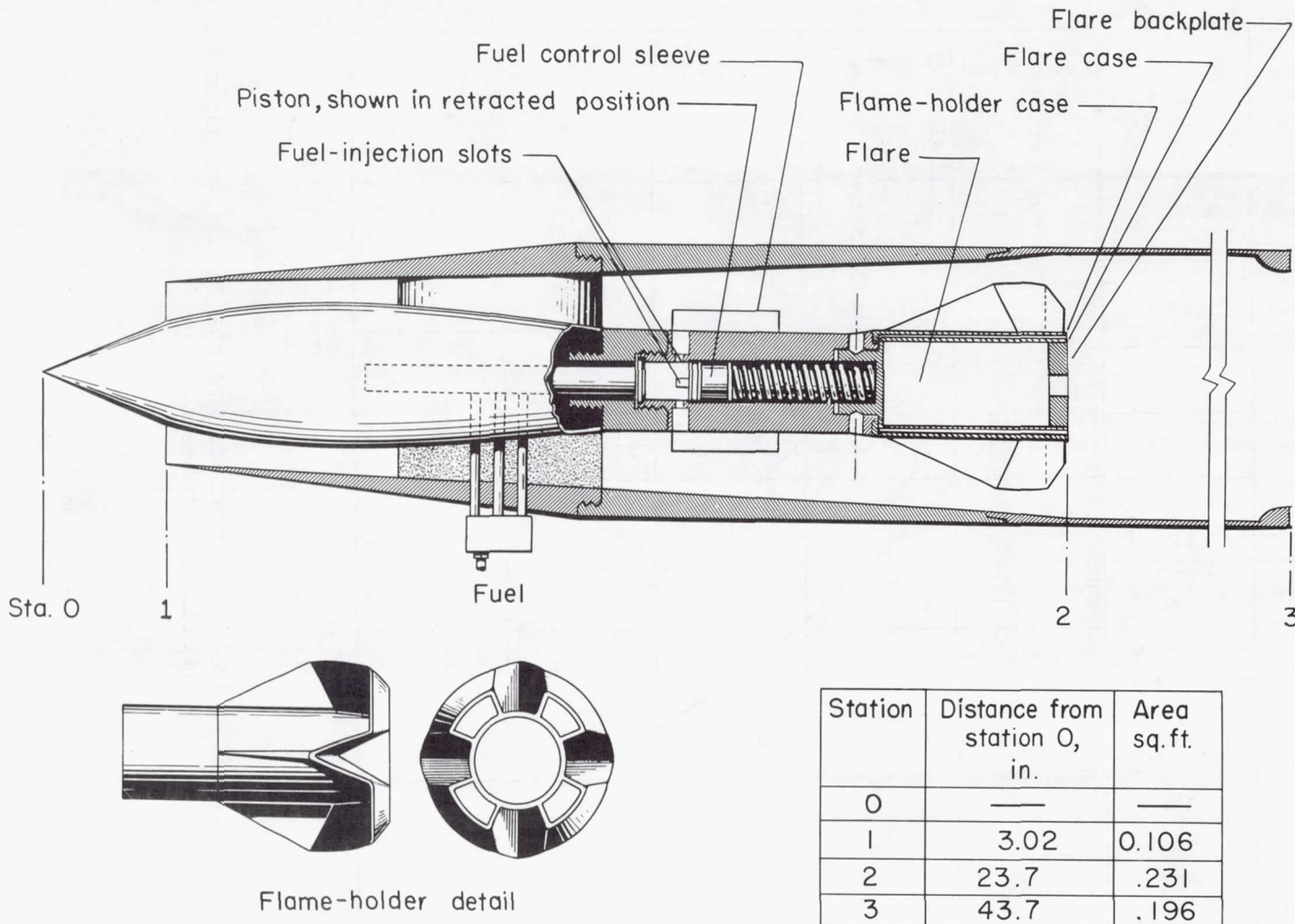
Figure 4.- The variation of ambient pressure and temperature with altitude.



L-76702

(a) Photograph of model mounted in  $M = 2.03$  free jet.

Figure 5.- The ram-jet engine used in preflight tests.



(b) Schematic drawing of the ram-jet engine.

Figure 5.- Concluded.

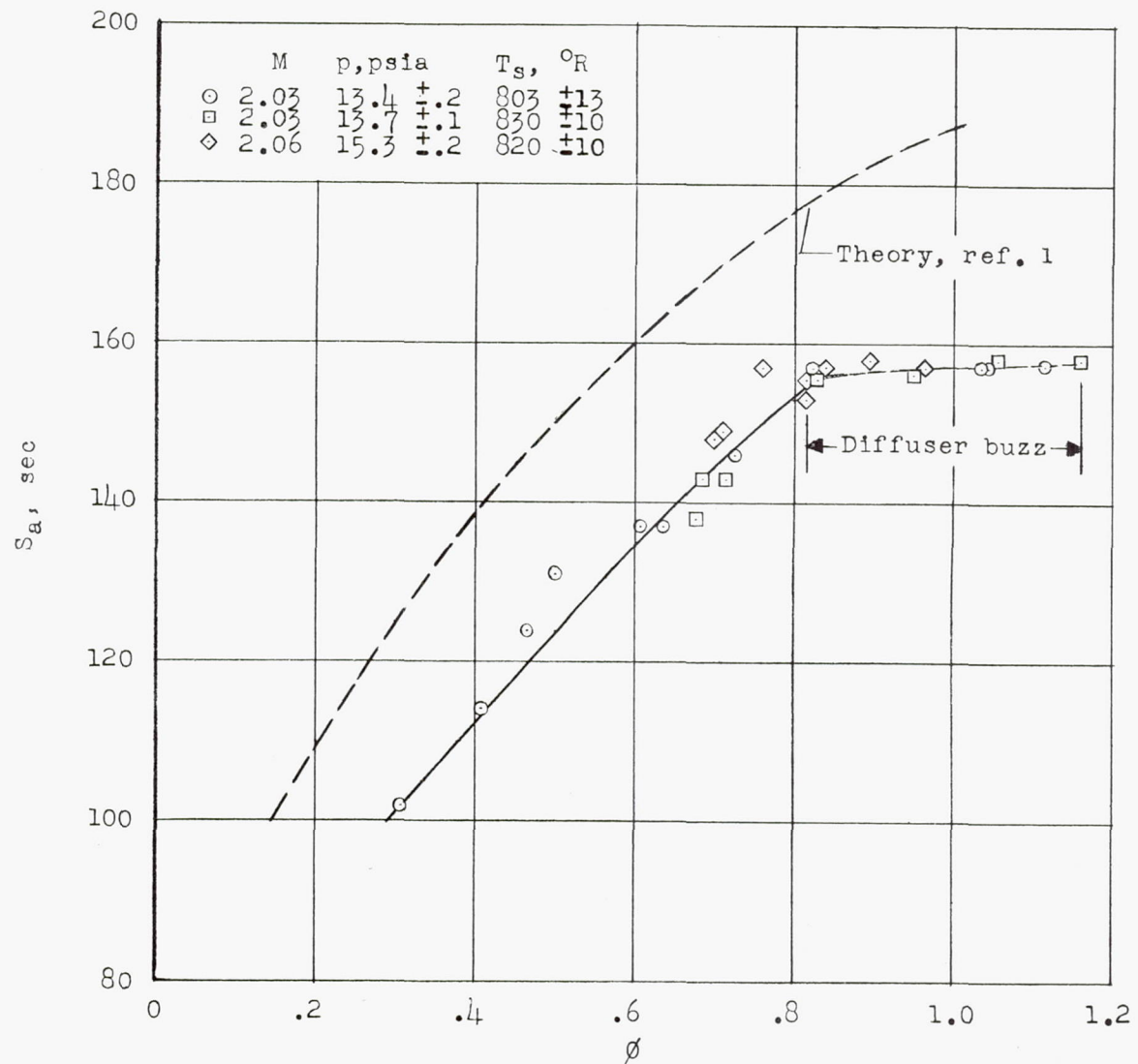


Figure 6.- Air specific impulse parameters for the fuel as obtained in preflight jet tests.

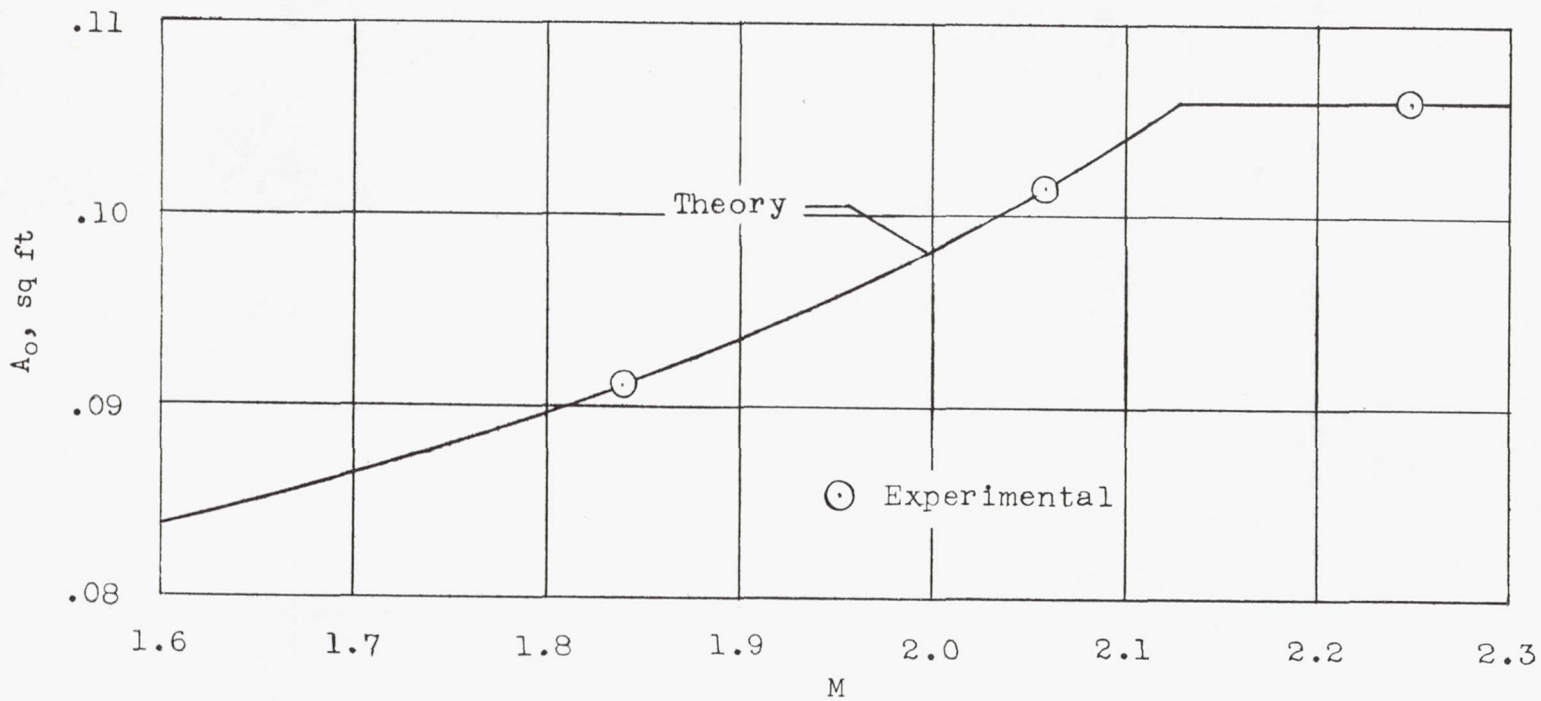


Figure 7.- The variation of maximum stream tube area with flight Mach number as determined from theory and ground tests by the methods of reference 7.

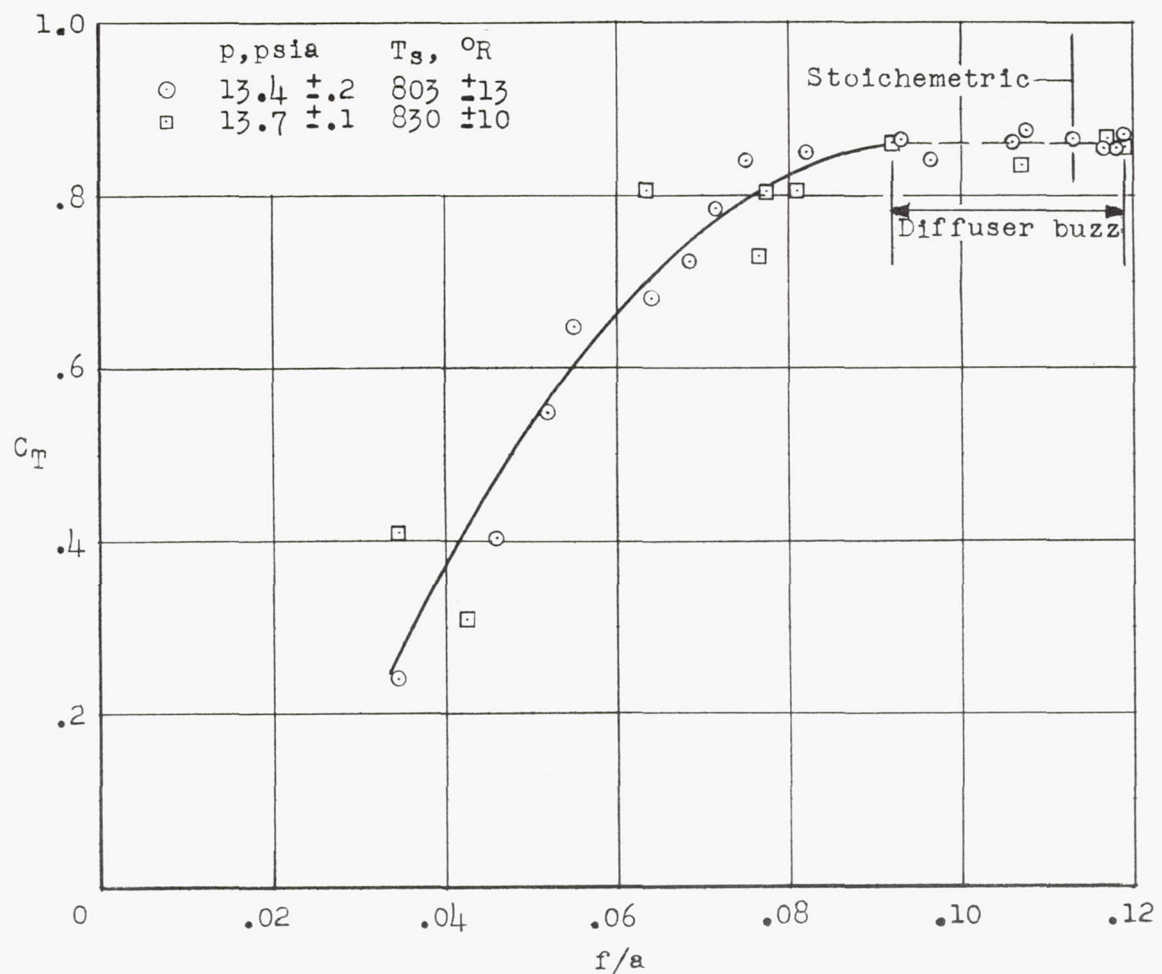


Figure 8.- Thrust characteristics of the slurry fuel ram-jet engine obtained in preflight jet tests at  $M = 2.03$ .

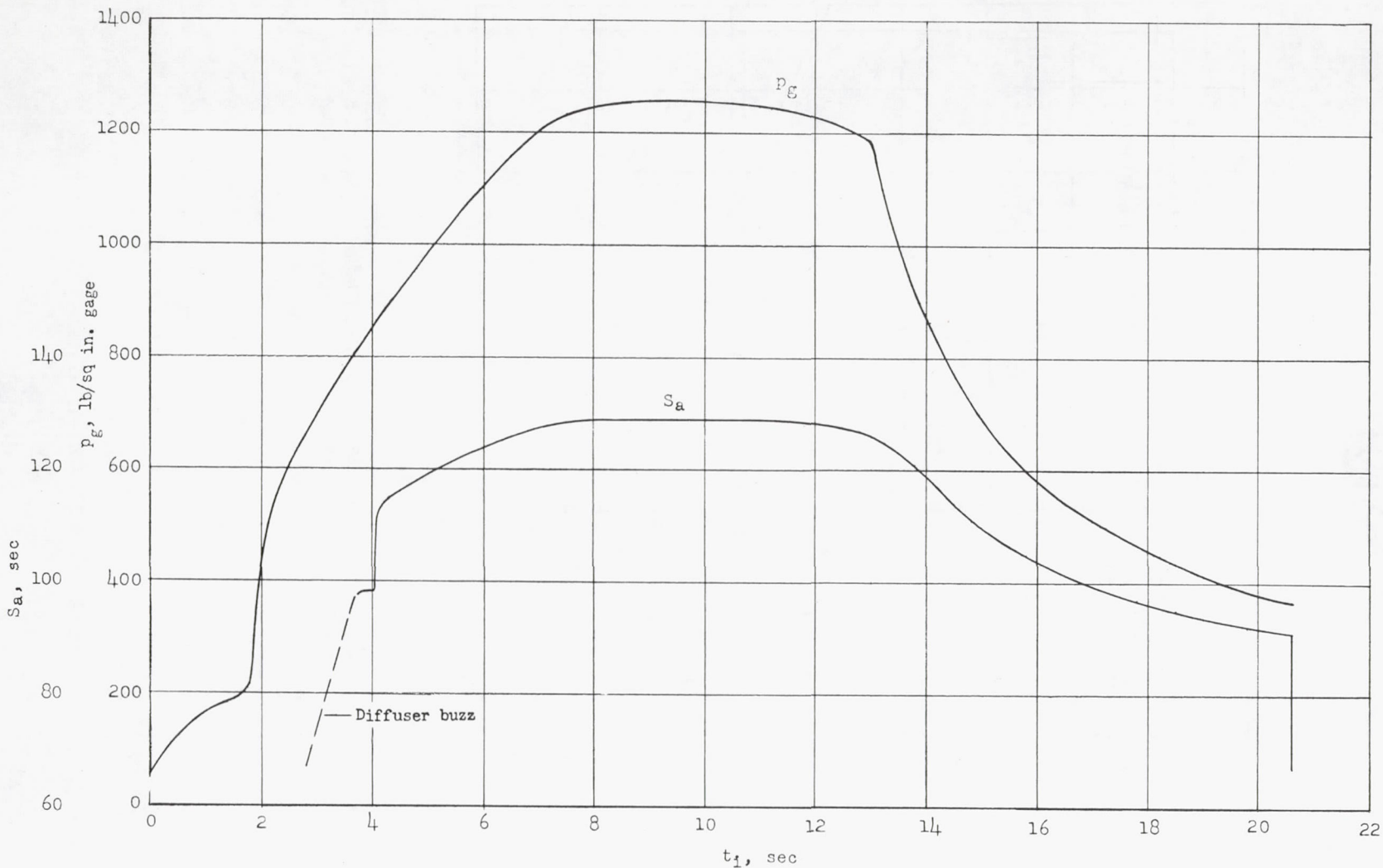


Figure 9.- A time history of air specific impulse and gas generator pressure as obtained in the preflight check of the flight test vehicle fuel system at  $M = 2.03$ .

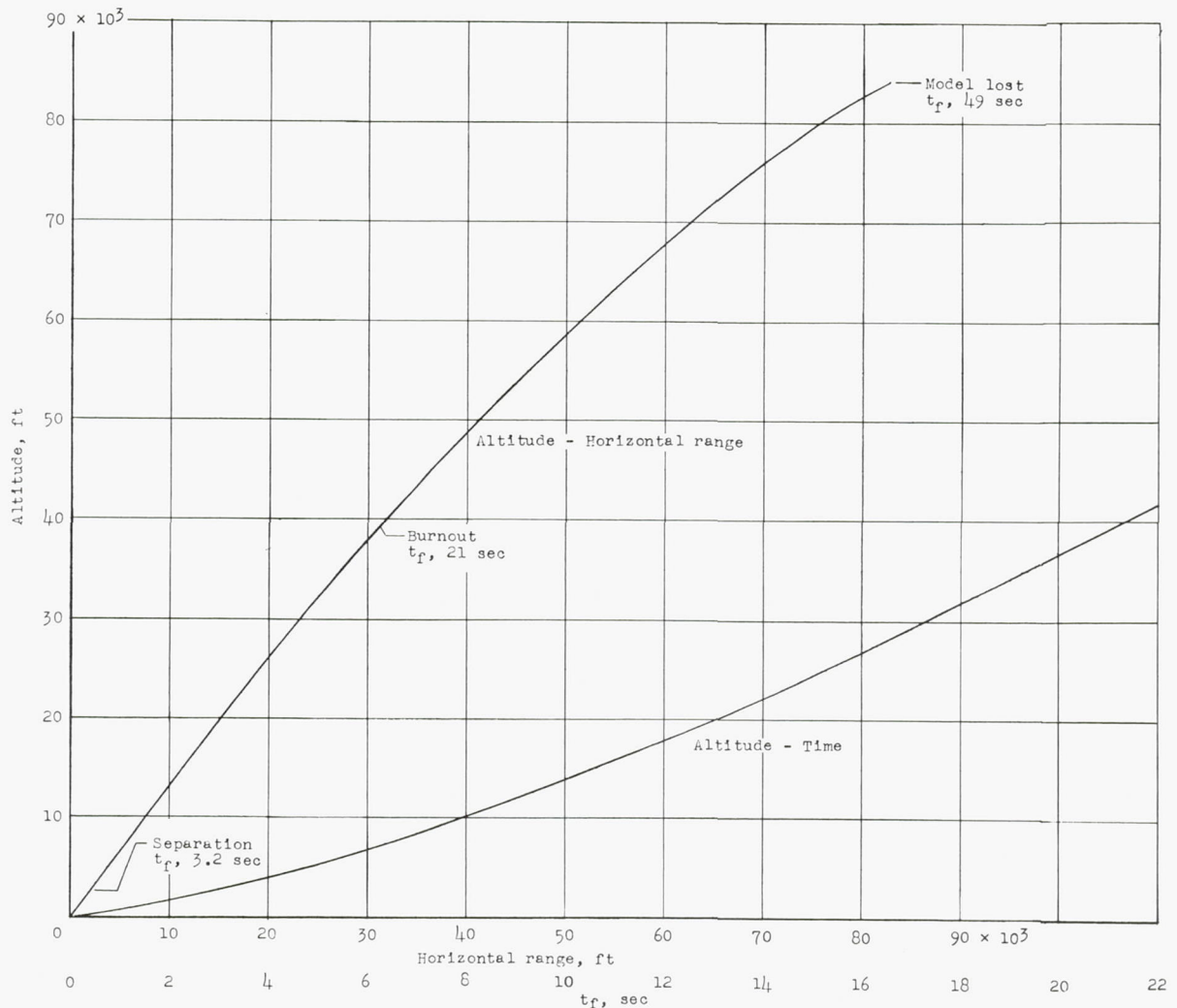


Figure 10.- The variation of altitude with horizontal range and flight time.

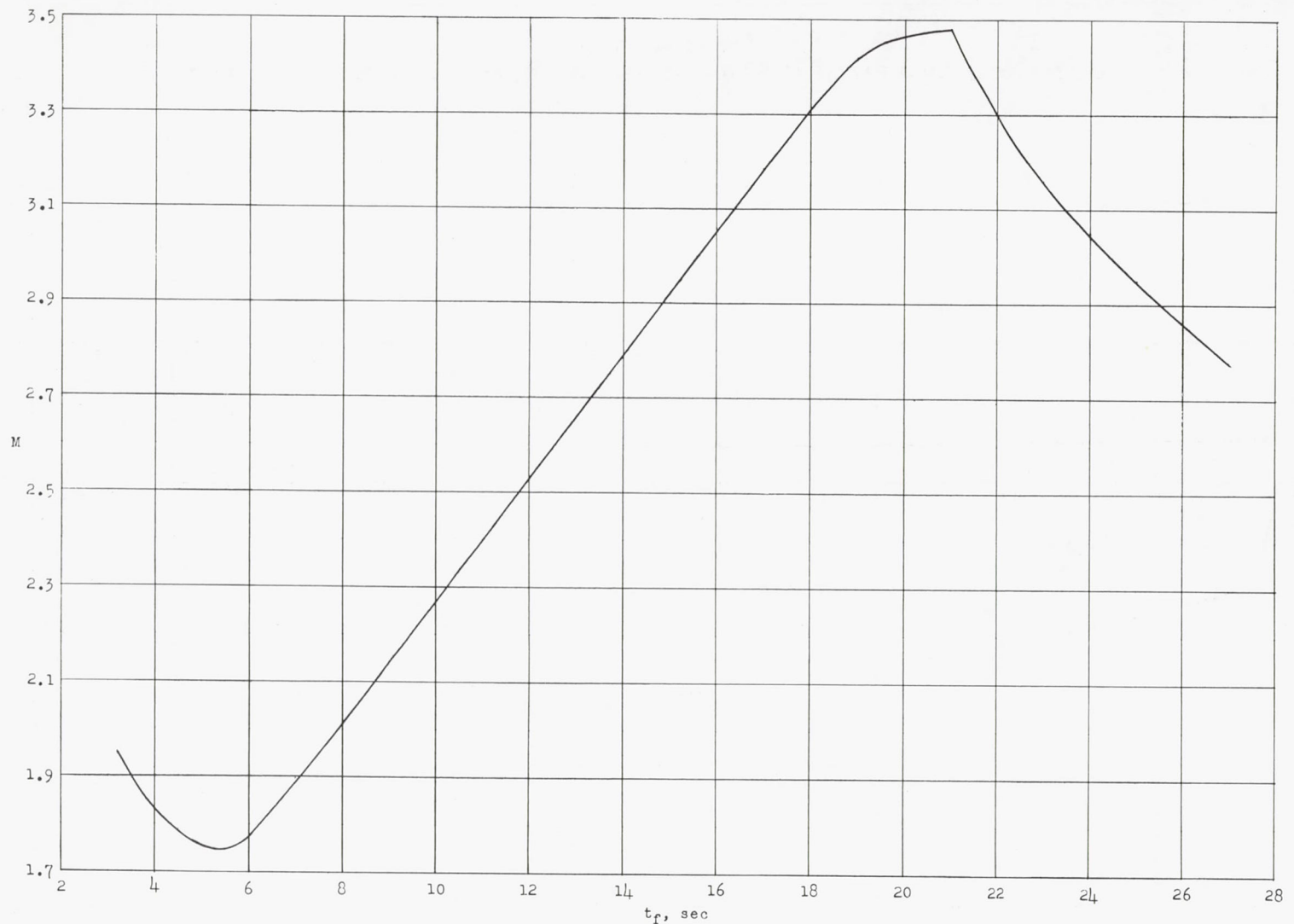


Figure 11.- The flight Mach number against time.

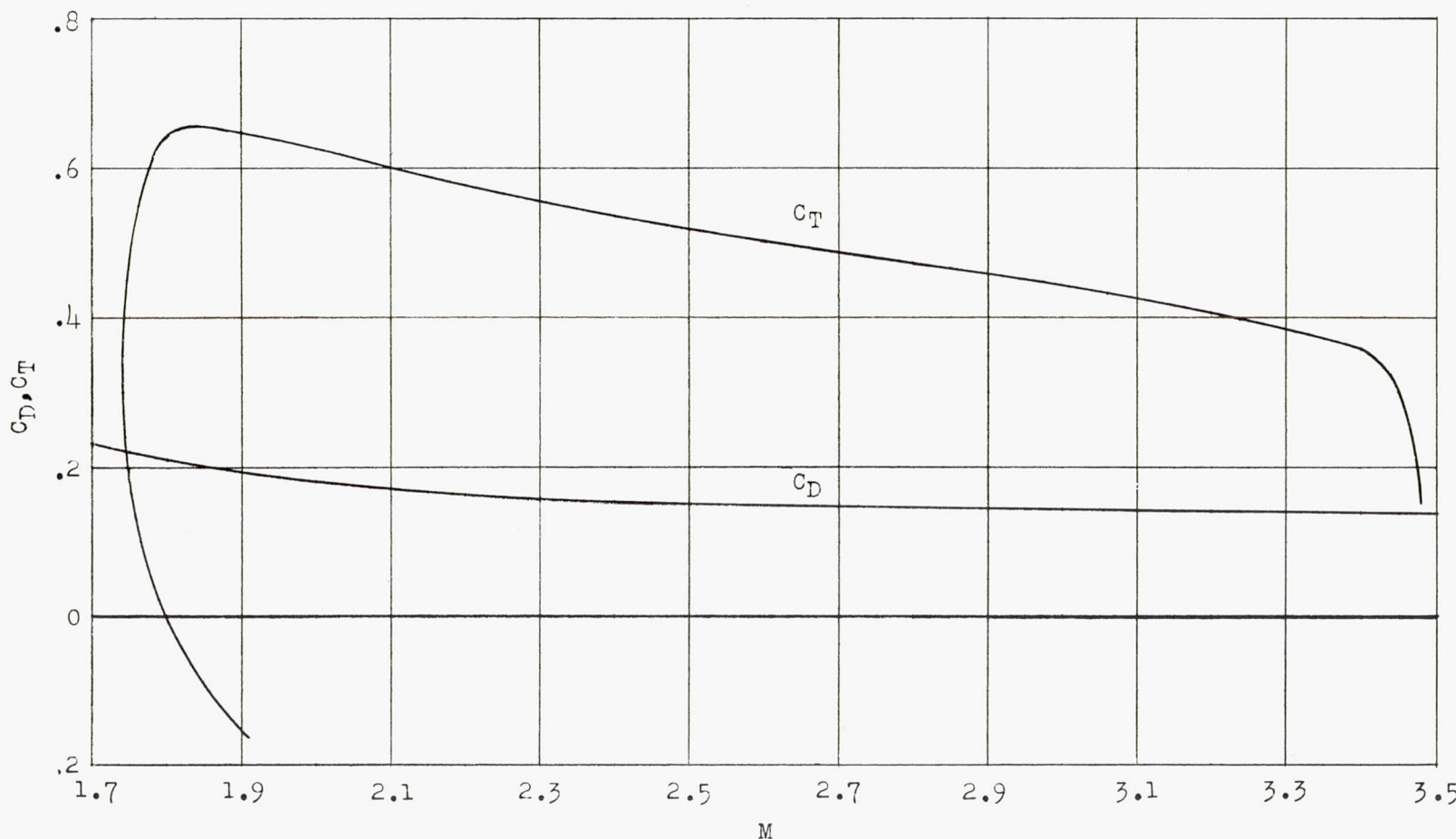


Figure 12.- The variation of thrust and drag coefficients with flight Mach number.

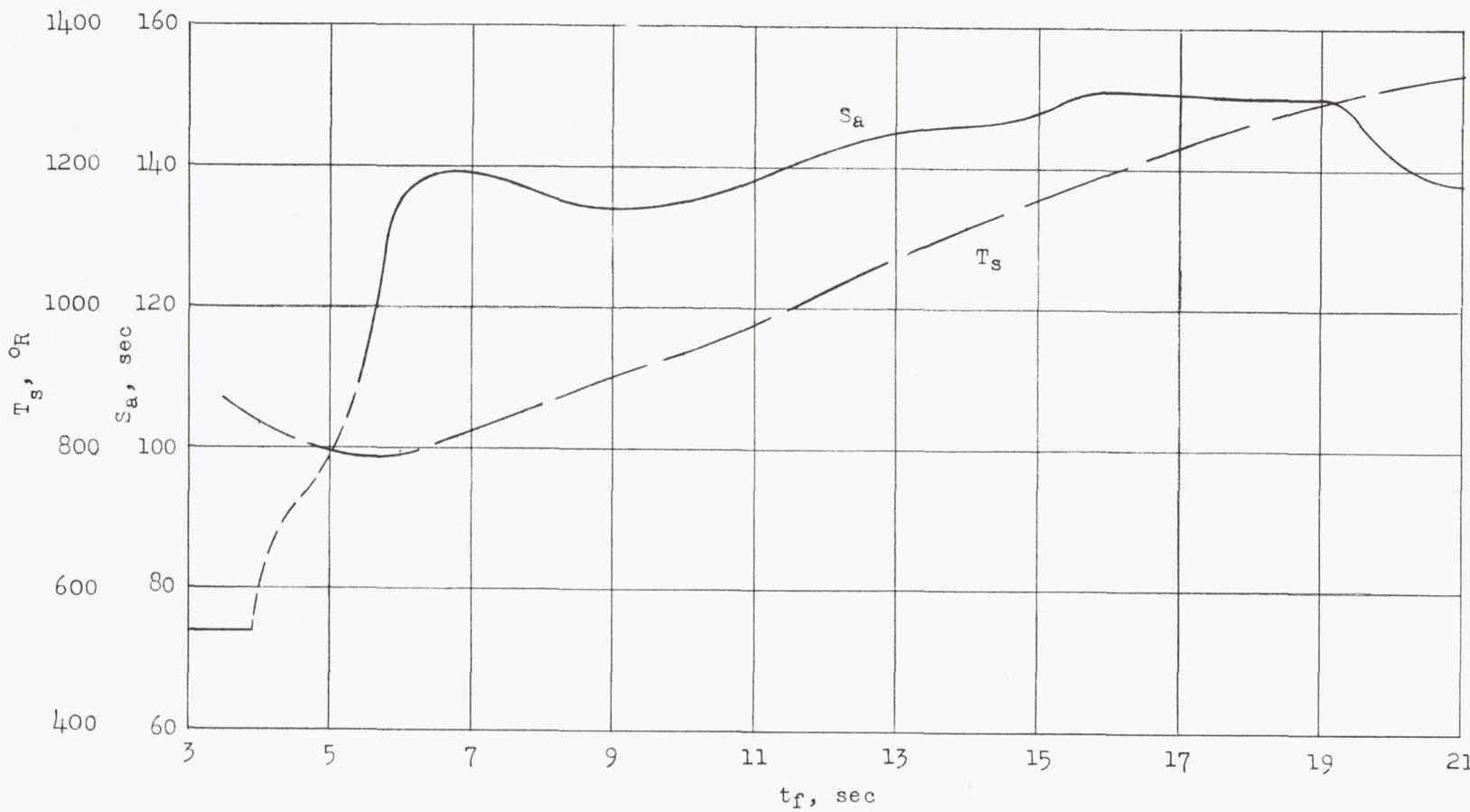


Figure 13.- The computed air specific impulse and stagnation temperature plotted against flight time.